The rainfall responses of Typhoon Soudelor (2015) to radiative processes of cloud species

Bin Wang

School of Earth Sciences, Zhejiang University, Hangzhou, Zhejiang, China

E-mail: beanwang@zju.edu.cn

In this study, five sensitivity experiments (Table 1) are conducted to investigate the radiative effects of cloud water, raindrop, cloud ice, snow, and graupel on rainfall of Typhoon Soudelor (2015), respectively.

Table 1 The design of sensitivity experiments.

Experiment	Explanation
CTL	Radiative effects of clouds on rainfall
NCR	Radiative effects of cloud water is excluded
NRR	Radiative effects of raindrops is excluded
NIR	Radiative effects of cloud ice is excluded
NSR	Radiative effects of snow is excluded
NGR	Radiative effects of graupel is excluded

The radiative effects of cloud ice and snow on rainfall are larger than those of three other cloud species (Table 2).

Table 2 Time means of changes in surface rain rate (P_S), net condensation (Q_{NC}) and hydrometeor change/convergence (Q_{CM}) from NCR, NRR, NIR, NSR and NGR to CTL averaged over the study area (Unit: mm d^{-1}).

	P_S	Q_{NC}	Q_{CM}
CTL-NCR	0.088	0.471	-0.383
CTL-NRR	-0.255	0.279	-0.535
CTL-NIR	-4.139	-4.665	0.525
CTL-NSR	2.801	2.526	0.273
CTL-NGR	0.131	0.012	0.118

This result corresponds to the changes in heat tendency due to radiation from NCR, NRR, NIR, NSR and NGR to CTL (Fig. 1). And the opposite effects of cloud ice and snow stem from the difference in vertical distribution between themselves (Fig. 2).

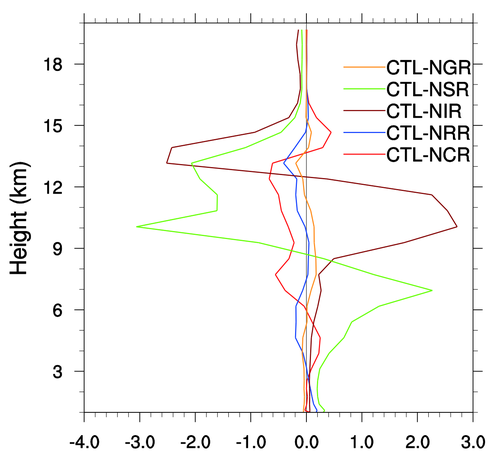

Fig. 1 Vertical profiles of differences in heat tendency due to radiation (°Cd^{-1}) between the control experiment and sensitivity experiments.

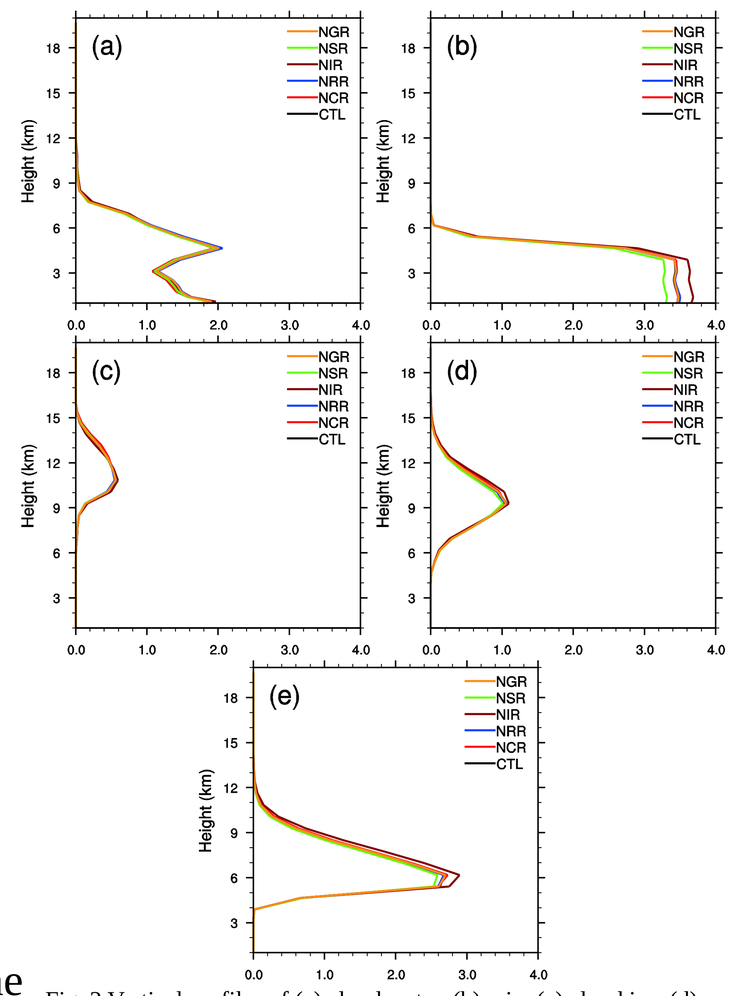

Fig. 2 Vertical profiles of (a) cloud water, (b) rain, (c) cloud ice, (d) snow and (e) graupel simulated in the control and sensitivity experiments. Unit is gkg^{-1}.

Since net condensation is related to release of latent heat in the heat budget and radiative heating/cooling also is a term in the heat budget, the radiative effects on heat budget are analyzed. $F_{loc}=F_{hd}+F_{rad}+F_{pbl}+F_{mp}$. Here, local heat change (F_{loc}) is associated with divergence of heat flux (F_{hd}), radiation (F_{rad}), sensible heat from the Planetary boundary layer (F_{pbl}) and latent heat (F_{mp}).

The analysis of heat budget reveals that the difference in release of latent heat is mainly balanced by the difference in divergence of heat flux below 12 km from NIR to CTL and below 9 km from NSR to CTL (Fig. 3).

The divergence of heat flux can be written as $F_{hd}=xytend+ztend$. Here, *xytend* and *ztend* are the divergence of horizontal and vertical heat flux, respectively. Figure 4 shows that the divergence of vertical heat flux is more important.

Decompose ztend into $ztend=ztend1+ztend2+ztend3$. Here, $ztend2 = F_\theta F_{d\omega,}$ where F_θ is mean temperature, and $F_{d\omega}$ is mean vertical divergence. Figure 5 shows that the differences in *ztend2* between the control experiment and sensitivity experiments are associated with those in vertical divergence.

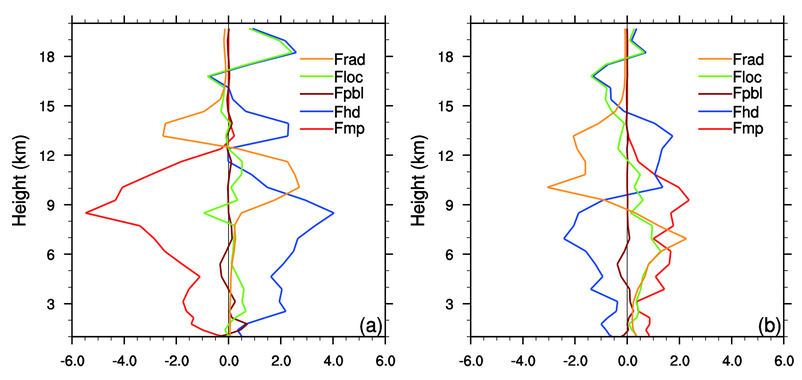

Fig. 3 Vertical profiles of differences in local temperature change (F_{loc}), divergence of heat flux (F_{hd}), sensible heat (F_{pbl}), latent heat (F_{mp}), and radiation (F_{rad}) for (a) CTL-NIR and (b) CTL-NSR. Unit is °C d^{-1}.

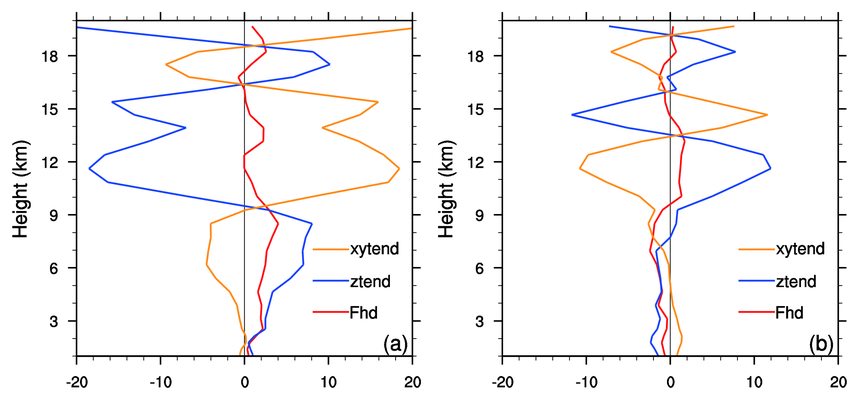

Fig. 4 Vertical profiles of differences in convergence of heat flux (F_{hd}) and its horizontal and vertical components (*xytend* and *ztend*, respectively) for (a) CTL-NIR and (b) CTL-NSR. Unit is °C d^{-1}.

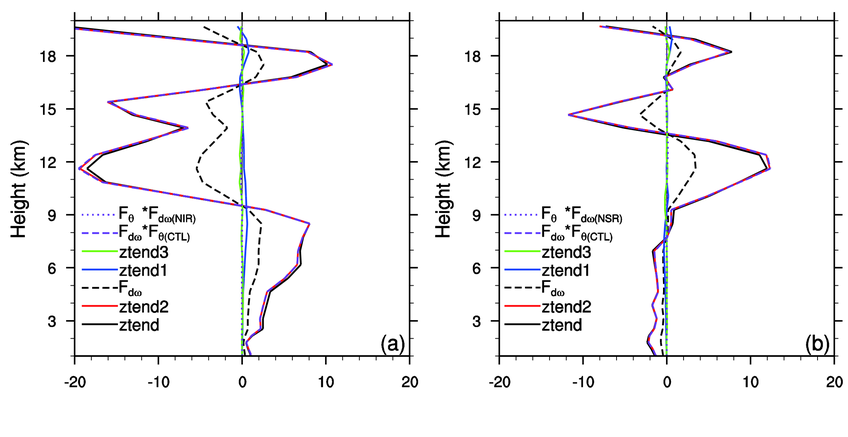

Fig. 5 Vertical profiles of components in *ztend* (°C d^{-1}): interaction between mean temperature and mean vertical divergence (*ztend*2; °C d^{-1}), vertical divergence (; 10^{-2} d^{-1}), mean vertical temperature advection (*ztend*1; 10^{-1}°C d^{-1}), and divergence of perturbation vertical heat flux (*ztend*3; °C d^{-1}) for (a) CTL-NIR and (b) CTL-NSR. The breakdowns of *ztend2* are $F_{d\omega}{}^{*}F_{\theta(CTL)}$ and $F_\theta{}^{*}F_{d\omega(NIR)}$ for (a) CTL-NIR and $F_{d\omega}{}^{*}F_{\theta(CTL)}$ and $F_\theta{}^{*}F_{d\omega(NSR)}$ for (b) CTL-NSR.

Summary

Since snow has its peak within the troposphere (around 9 km), the enhanced radiative cooling by emiting more longwave radiation in the upper troposphere and the suppressed radiative cooling by trapping more longwave radiation in the lower troposphere resulting from the inclusion of radiative effects of snow increases instability and thus vertical mass divergence and divergence of heat flux below the height of ice hydrometeor peak. As a result, the enhanced release of latent heat corresponds to the strengthened divergence of heat flux, increasing net condensation and rainfall.

The peak of cloud ice appears around the tropopause (around 11 km), the suppressed radiative cooling in the upper troposphere caused by the inclusion of radiative effects of cloud ice increases stability and thus decreases vertical mass divergence and divergence of heat flux. Thus, the suppressed release of latent heat corresponds to the weakened divergence of heat flux, decreasing net condensation and rainfall.

(Xu et al. 2016, *J. Geophys. Res. Atmos.*, 121,14,127–14,136, doi:10.1002/2016JD025479.)